

## Photonic Hall effect of inactive Mie scatterers in a Faraday active matrix

G. Düchs,<sup>1</sup> A. Sparenberg,<sup>1</sup> G. L. J. A. Rikken,<sup>1</sup> and B. A. van Tiggelen<sup>2</sup>

<sup>1</sup>*Grenoble High Magnetic Field Laboratory, Max Planck Institut für Festkörperforschung/CNRS, Boîte Postale 166, 38042 Grenoble Cedex 9, France*

<sup>2</sup>*Laboratoire de Physique et Modélisation des Milieux Condensés/CNRS, Maison des Magistères, Université Joseph Fourier, Boîte Postale 166, 38042 Grenoble Cedex 9, France*

(Received 28 January 2000)

We describe an experimental study of the photonic Hall effect in media consisting of a magneto-optically active matrix and magneto-optically inert Mie scatterers. We call such media reversed with respect to the normal media having magneto-optically active Mie scatterers in inert matrices in which the photonic Hall effect has been studied so far. We show the photonic Hall effect in reversed media to be proportional to  $VB\ell^*$ , where  $V$  is the Verdet constant of the matrix,  $\ell^*$  the transport mean free path of the liquid, and  $B$  the applied magnetic field. We further propose an empirical expression that unifies the results obtained in normal and reversed media and present a simple analytic model to illustrate the photonic Hall effect.

PACS number(s): 42.25.Bs, 42.68.Mj

Recently it was shown both theoretically [1,2] and experimentally [3,4] that light diffusing in a disordered medium subject to a magnetic field can show behavior that bears a strong phenomenological resemblance to the well-known solid-state electronic magnetotransport effects [5]. In particular, the electronic Hall effect and magnetoresistance were found to have photonic analogs. There is, however, an important conceptual difference. The origin of the electronic effects lies in the Lorentz force that causes a deflection of the electron trajectories between scattering events. On the other hand, most of the photonic counterparts considered so far find their origin in the magnetically induced changes of the optical properties of the scatterers and no magnetic-field influence occurs on light propagation between scatterers. Here, we present experiments on the photonic Hall effect in reversed media, i.e., in media consisting of scatterers with negligible magneto-optical activity embedded in a matrix that is magneto-optically active. As the influence of an external magnetic field on the photon propagation now mainly occurs in the matrix between the scatterers, light diffusion in such a medium constitutes a closer analogy to diffusive electronic magnetotransport. In the following we shall briefly sketch the theoretical background (Sec. I), we then present our experimental results (Sec. II) followed by a discussion (Sec. III), and finally we describe a simple model to illustrate the effect (Sec. IV).

### I. THEORETICAL BACKGROUND

Maxwell's equations plus the known magneto-optical material parameters in principle offer the possibility to exactly calculate the effect of a magnetic field on the diffusion of light in strongly disordered media. In practice this is, however, completely impossible, and theoretical simplifications have to be made, as was first done in Refs. [1] and [2]. Recently, the photonic Hall effect was calculated for magnetoactive Mie particles [6] providing support for the experiments reported in Ref. [3]. The effect of a static magnetic field  $\mathbf{B}$  on the optical properties of an isotropic nonabsorbing

medium is described by the refractive index tensor  $n(\mathbf{B})$ , given up to first order in  $\mathbf{B}$  by [7]

$$n_{ij}(\mathbf{B}) = n \delta_{ij} + i \frac{V}{k} \epsilon_{ijk} B_k, \quad (1)$$

where  $k$  is the vacuum wave vector and  $n$  is the refractive index of the medium. The Verdet constant  $V$  determines the strength of magnetic circular birefringence (Faraday effect). Our present experiment deals with scatterers made of magneto-optically inactive ( $V_s \approx 0$ ) material with refractive index  $n_s$ . They are randomly distributed with a volume fraction  $f$  in an isotropic matrix with refractive index  $n_m$  and  $V_m \neq 0$ . If the transport mean free path of the light  $\ell^*$  is much smaller than the geometrical dimensions of the scattering ensemble, the propagation of light is diffuse and can be characterized by a second-rank diffusion tensor  $D_{ij}$  relating the diffuse photon flux density to the gradient of the photon density. This tensor can be expressed as [2]

$$D_{ij}(\mathbf{B}) = D_0 \delta_{ij} + D_H \epsilon_{ijk} B_k + \Delta D_{\perp} (B^2 \delta_{ij} - B_i B_j) + \Delta D_{\parallel} B_i B_j, \quad (2)$$

where  $D_0$  describes conventional isotropic diffusion,  $D_H$  magnetotransverse diffusion, and  $\Delta D_{\perp, \parallel}$  magnetoresistance, observable in transmission perpendicular and parallel to the magnetic field, respectively. The magnetic-field dependence of the refractive index of the matrix is responsible for the magnetic-field dependence of this diffusion tensor. The existence of the Hall-type term  $D_H$  and of the magnetoresistance term  $\Delta D_{\perp}$  have been verified experimentally for the case of magnetoactive scatterers in an inert matrix [3,4].

In our previous work it was found that the effect of the magnetic field on the diffusion of light can be described by the dimensionless parameter  $VB\ell^*$  [8]. In large magnetic fields, the parameter  $VB\ell^*$  can approach unity [9], but all our experiments obey  $VB\ell^* \ll 1$ . The quantity  $VB\ell^*$  determines the average number of (Faraday) rotations of the electric polarization vector of the photons between subsequent scattering events. The same parameter was seen to be important for the suppression of coherent backscattering in magnetic fields, both experimentally [9,10] and numerically [11].

An analogous situation occurs in diffusive electronic magnetotransport. There, the magnetic-field effect is determined by the dimensionless parameter  $\omega_c \tau$ , where  $\omega_c$  is the cyclotron frequency and  $\tau$  the scattering time. This equals the average number of cyclotron orbits that an electron completes between two scattering events. Simple free-electron models show that the resulting Hall angle is proportional to  $\omega_c \tau$  and that the longitudinal electronic magnetoresistance is proportional to  $(\omega_c \tau)^2$  [5]. Also in the case of the Beenakker-Senftleben effect [12], i.e., the magnetic-field dependence of the thermal conductivity of gases, an analogous parameter has been established, namely the number of spin precessions between molecular collisions.

## II. EXPERIMENTAL RESULTS

For the experimental observation of the photonic Hall effect in reversed media, a matrix with a large Verdet constant  $V$  is required. This can be found in materials containing large concentrations of paramagnetic rare-earth ions such as  $\text{Ce}^{3+}$  or  $\text{Dy}^{3+}$ . In such materials,  $V$  is negative and inversely proportional to temperature. Its absolute value can thus be further increased by cooling. Furthermore, the matrix should be amorphous, isotropic, and nonabsorbing. We have found two different matrices that fulfill all these requirements: a saturated aqueous dysprosium chloride solution and a dysprosium nitrate glass. The solution was prepared by dissolving 1.8 g/ml  $\text{DyCl}_3 \cdot 6\text{H}_2\text{O}$  in water. This solution is transparent apart from a few narrow and weak  $4f$ - $4f$  transitions of the  $\text{Dy}^{3+}$  ion. The present measurements were done far from these absorption bands. The refractive index  $n_m(\text{sol})$  of the solution was found to be 1.44 at a wavelength of 457 nm. The Verdet constant at this wavelength is  $-90$  rad/T m at 77 K. The nitrate glass was prepared by melting a mixture of  $\text{Dy}(\text{NO}_3)_3 \cdot 5\text{H}_2\text{O}$  and  $\text{DyCl}_3 \cdot 6\text{H}_2\text{O}$  (10:1 wt/wt) at 420 K, followed by rapid cooling to room temperature, upon which a clear, stable glass is obtained. Its refractive index  $n_m(\text{glass})$  was found to be 1.53 at 457 nm and its Verdet constant is  $-59$  rad/T m at 300 K. Scattering samples were prepared by adding  $\text{Al}_2\text{O}_3$  particles to the matrix. The refractive index  $n_s$  of these particles is 1.77 at 457 nm. Their average diameter was  $1 \mu\text{m}$  with a 50% size dispersion, putting them in the Mie regime. Scatterer volume fraction  $f$  ranged between 0.01 and 0.1, which means that we deal with dilute samples. The transport mean free path  $\ell^*$  of the light in these scattering media has been determined by measuring their optical transmission  $T$  by means of an integrating sphere and using  $T = 1.6\ell^*/L$ , where  $L$  is the sample thickness [15]. Figure 1 shows  $\ell^*$  as a function of  $f^{-1}$  for the solution samples, confirming the expected behavior for dilute samples.

The photonic Hall effect was measured by phase-sensitive detection of the magnetically induced changes in the difference between the light intensities scattered to the left- and to the right-hand side of the magnetic field (see Fig. 2). Monochromatic illumination at 457 nm was provided by an argon-ion laser and guided to the sample by an optical fiber (diameter 1 mm, numerical aperture 0.5). The light incident on the sample was unpolarized. The scattered light was collected again by optical fibers (same type) and measured with silicon photodiodes. An alternating magnetic field  $B(t) = B \cos \Omega t$

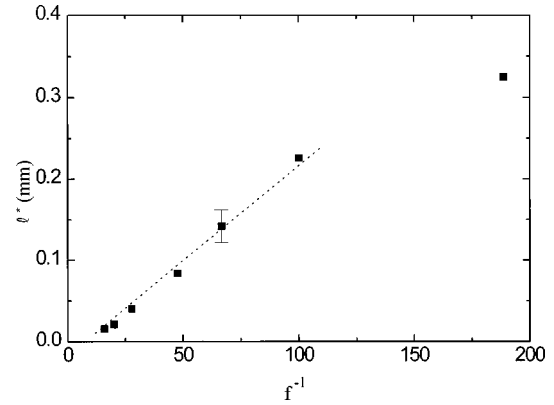


FIG. 1. Transport mean free path  $\ell^*$  as a function of the inverse volume fraction of scatterers  $f$  for the solution samples at  $\lambda = 457$  nm. The straight line is meant to guide the eye.

with  $B \approx 1$  T and  $\Omega \approx 30$  Hz was applied perpendicular to the illuminating and collecting light guides. Samples were cylindrical, with the axis parallel to the illuminating fiber, and with a diameter of 1 mm and a length of 1.5 mm. In this way, the magnetotransverse photon flux  $\Delta I_{\perp} \equiv I_L - I_R$  is obtained which is then normalized by the transversely scattered intensity  $I_{\perp} \equiv (I_L + I_R)$ . This ratio is proportional to the ratio of the magnetotransverse and normal diffusion coefficients, given in Eq. (2), and can be considered to be a photonic analog of the Hall angle in electronic magnetotransport. Figure 3 shows that  $\Delta I_{\perp}/I_{\perp}$  depends linearly on the magnetic field which leads us to define a  $B$ -normalized photonic Hall angle by  $\eta \equiv \Delta I_{\perp}/(I_{\perp} B)$ . This quantity is a characteristic for any given scattering sample. We found that the sign of the photonic Hall effect in reversed media with a paramagnetic matrix ( $V_m < 0$ ) is the same as the one obtained for normal media with paramagnetic scatterers ( $V_s < 0$ ). The temperature dependence implied by Fig. 3 is explicitly shown in Fig. 4. As the only temperature-dependent parameter in the scattering process is the Verdet constant  $V$

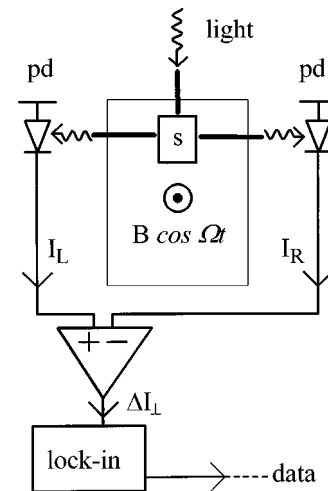


FIG. 2. Schematic setup of the photonic Hall effect measurement: The sample ( $s$ ) is situated in an alternating magnetic field. The light scattered perpendicular to both the incident light beam and the magnetic field is detected by two photodiodes (pd). The magnetotransverse photon flux  $\Delta I_{\perp} = I_R - I_L$  is detected with a lock-in amplifier.

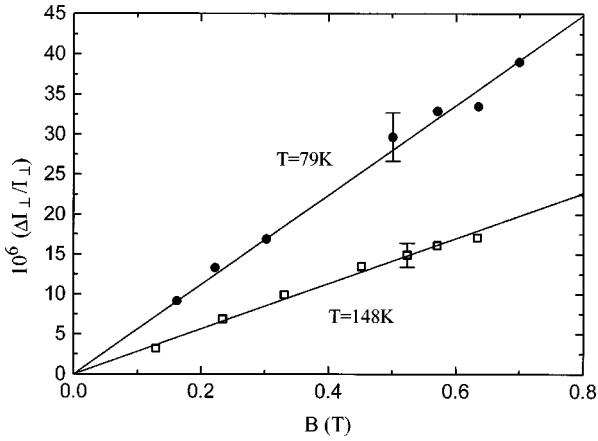


FIG. 3. Normalized magnetotransverse photon flux as a function of magnetic-field amplitude for a solution sample with  $f=0.042$  at two temperatures. Straight lines are fits through the origin.

$\propto T^{-1}$ , the observed linear dependence on the inverse temperature confirms the linear relation between the normalized photonic Hall angle and the Verdet constant.

The effect of scatterer concentration on the photonic Hall angle is shown in Fig. 5 for both solution and glass samples. In view of the small scatterer concentrations  $f$  in all the samples, the effective Verdet constant of the medium  $V_{\text{eff}} \approx (1-f)V_m$  can be considered the same for the samples in each of these curves whereas the scattering mean free path  $\ell^*$  being proportional to  $1/f$  changes considerably. The two curves in Fig. 5 are very similar; upon decreasing the scatterer volume fraction, an increase in the normalized photonic Hall angle is observed, until at a low volume fraction the photonic Hall angle decreases and even changes sign. In the multiple scattering regime [i.e., for  $f \geq 0.02$  in Fig. 5(a) and  $f \geq 0.05$  in Fig. 5(b), respectively], this curve reveals a linear dependence of the photonic Hall angle on the mean free path in the samples. Figure 6 explicitly shows the linear dependence on the transport mean free path in this regime. This does not hold any longer when the volume fractions are smaller, i.e., when the transport mean free path becomes comparable to the size of the sample. For the single scattering regime at very low volume fractions, the sign of the

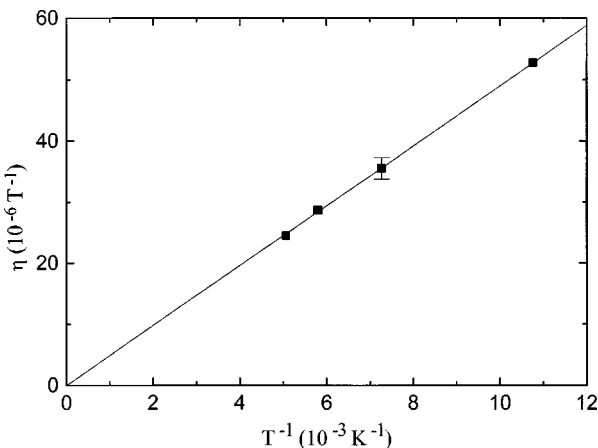


FIG. 4. Temperature dependence of the  $B$ -normalized photonic Hall angle  $\eta$  for a solution sample with  $f=0.042$ . The straight line is a fit through the origin.

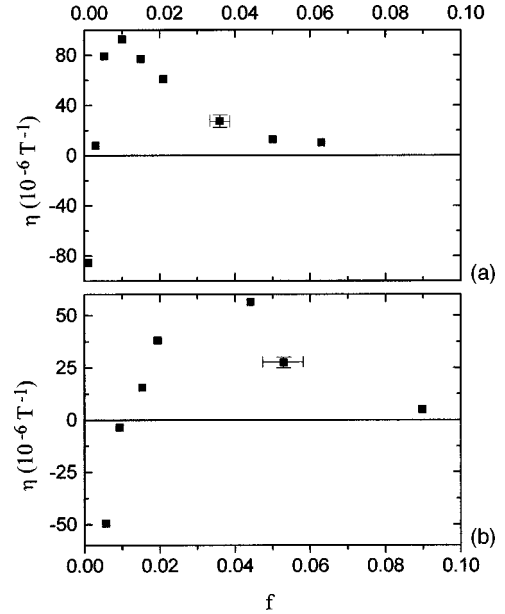


FIG. 5. Normalized photonic Hall angle  $\eta$  as a function of scatterer volume fraction  $f$  for solution samples at 77 K (top panel) and glass samples at 300 K (bottom panel). At the very left, one is in the single scattering regime; the multiple scattering regime begins at about the maximum of each curve.

magnetotransverse photon flux is opposite (Fig. 5). Since the refractive index difference between scatterer and matrix is smaller for the glass samples and therefore the same transport mean free path corresponds to higher scatterer concentrations, this turnover occurs at higher  $f$  in the glass samples [Fig. 5(a)] than in the solution samples [Fig. 5(b)].

### III. DISCUSSION

The change of sign of the magnetotransverse photon flux between the multiple and the single scattering regime (Fig. 5) is quite remarkable. (In the single scattering regime, one should speak about the magnetotransverse photon flux and not about a photonic Hall effect as there is no diffuse photon transport in this regime.) This change of sign was not found

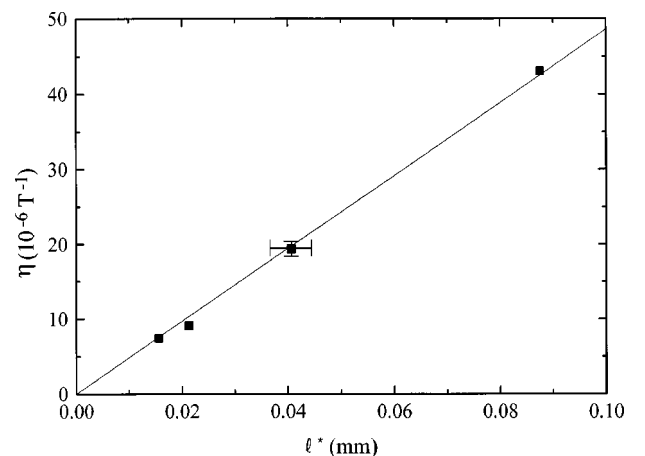


FIG. 6. Normalized photonic Hall angle  $\eta$  as a function of the transport mean free path  $\ell^*$  for solution samples at 77 K in the multiple scattering regime.

in previous measurements in normal media [3], and theory does not predict it either for normal media [6]. Why it occurs in reversed media is not yet well understood. In any case, it seems clear that for volume fractions around  $f \approx 0.5$ , there is no meaning in differentiating between scatterers and matrix and the photonic Hall angle should have the same sign for both normal and reversed media. This is in agreement with the fact that for the higher volume fractions we got the same sign as in normal media.

In the multiple scattering regime, the photonic Hall effect was found proportional to the transport mean free path  $\ell^*$  (Fig. 6). In the last part of this paper, we will describe a simple model for the photonic Hall effect in reversed media. In this model, the photonic Hall effect is due to a magnetically induced change of interference between photons that have traveled different paths in the magneto-optically active matrix around the scatterers. In this respect, the model for reversed media is different from a similar model that has been proposed for the photonic Hall effect in normal media and where the photonic Hall effect is only due to a magnetically induced change in the scattering cross section of the individual scatterers [14]. From the model for reversed media, we assume a  $VB\ell^*$  dependence of the photonic Hall effect, which is in accordance with our experimental results.

The observation of the photonic Hall effect in reversed media further strengthens the phenomenological analogy between photonic and electronic magnetotransport. The reversed medium is mathematically more difficult to handle and no theoretical description of diffusive photon transport is yet available. Intuitively, it will be clear that the photonic Hall effect in normal and reversed media should be related. For normal media, it has been proposed [3,8] that the photonic Hall angle may be proportional to  $V_{\text{eff}}B\ell^*$ , where  $V_{\text{eff}} = fV_s$ . We emphasize that this formula is not theoretically confirmed but is a phenomenological description of experimental results. Above, we have shown that for reversed media  $\Delta I_{\perp}/I_{\perp} \propto V_m B\ell^*$ . In order to give a unified description of these results, we propose an empirical expression for arbitrary two-component media in the multiple scattering regime:

$$\eta = N[fV_s + (1-f)V_m]\ell^*, \quad (3)$$

where  $N$  is a numerical factor that depends on the shape of the sample and the size of the scatterers and  $fV_s + (1-f)V_m$  is the effective Verdet constant of the scattering medium as a whole. Note that for the experiments described in this paper, the dependence of  $\eta$  on the scatterer fraction  $f$  (Fig. 5) only reflects its dependence on  $\ell^*$  (Fig. 6) and no direct influence of  $f$  on  $\eta$  has been found. But as  $(1-f) \approx 1$  in all these experiments, our results are still properly described by Eq. (3). Furthermore, all measurements done so far dealt with media where the refractive indices of scatterer and matrix were similar, i.e.,  $|m-1| < 1$ . Outside this region, the behavior of the photonic Hall effect might be much more complicated. For the reversed solution samples studied here, we find  $N = (5 \pm 2) \times 10^{-3}$ , and for normal samples consisting of Faraday active  $\text{CeF}_3$  Mie scatterers in an inert matrix in the same geometry and at the same wavelength, it has been found  $N = (4 \pm 2) \times 10^{-3}$  [16,3]. These values agree

within their error bars and all experimental results obtained so far may phenomenologically be described by Eq. (3).

#### IV. A SIMPLE MODEL

A basic understanding of the reversed photonic Hall effect can be found by considering the scattering cross section of one and two Rayleigh scatterers, respectively, embedded in a magneto-optical active matrix. An analogous model has already been considered for the normal case of magnetoactive scatterers in passive matrices [14]. We emphasize that this is a very simple model for what happens in multiple scattering and that it can only be regarded as an instructive illustration of the effect. Let us first treat the case of one scatterer at the origin.  $R$  is the distance from the particle and we assume that  $kR \gg 1$  (far field) and we will only deal with contributions in first order of  $B$ . In the Born approximation, the scattering matrix  $\mathbf{T}$  just equals the potential  $\mathbf{U} = (\mathbf{n}_m^2 - \mathbf{n}_s^2) \times (\omega^2/c^2)^{4/3} \pi a^3$ , where  $a$  is the scatterer diameter [13]. We approximate this by a constant potential  $U$ , which means that we neglect the influence of the magnetic field on the scattering processes, which is of the order of  $VB/k$  [cf. Eq. (1)]. The influence of the magnetic field will only be taken into account for the propagation of the scattered light in the Faraday active medium as was done in Ref. [11]. The scattering amplitude for one scatterer is proportional to

$$s(\mathbf{g}_{\text{in}}, \mathbf{k} \rightarrow \mathbf{g}_{\text{out}}, \mathbf{k}') \propto \mathbf{g}_{\text{in}}^*(\mathbf{k}) \cdot \mathbf{U} \mathbf{G} \cdot \mathbf{g}_{\text{out}}(\mathbf{k}') R, \quad (4)$$

where  $\mathbf{k}, \mathbf{k}'$  are the wave vectors of the ingoing and outgoing wave,  $\mathbf{g}_{\text{in}}, \mathbf{g}_{\text{out}}$  are their polarization vectors, and  $\mathbf{G}$  is the Green function for the Faraday active medium [2]:  $\mathbf{G}(k, \mathbf{p}, \mathbf{B}) = [k^2 \mathbf{I} + \mu \Phi - \Delta_{\mathbf{p}}]^{-1}$  with  $\Phi \equiv i(\boldsymbol{\varepsilon} \cdot \hat{\mathbf{B}})$ , where  $\boldsymbol{\varepsilon}$  is the third-rank antisymmetric Lévi-Civita tensor, and  $\mu = 2VBk$ .  $\Delta_{\mathbf{p}}$  projects upon the transverse plane perpendicular to the momentum  $\mathbf{p}$ . In real space and for  $VBR < 1$  and  $kR \gg 1$ ,  $\mathbf{G}$  may be written as

$$\mathbf{G}(k, \mathbf{R}, \mathbf{B}) = \mathbf{G}_0(k, \mathbf{R}) + \delta \mathbf{G}(k, \mathbf{R}, \mathbf{B}) + O(\mathbf{B}^2) \quad (5)$$

with  $G_0 = -\Delta_{\mathbf{R}}(e^{ikr}/4\pi R)$  and  $\delta \mathbf{G} = -(e^{ikr}/8\pi i)2VB[\Phi - \Phi \cdot \hat{\mathbf{R}}\hat{\mathbf{R}} - \hat{\mathbf{R}}\hat{\mathbf{R}} \cdot \Phi + (i/kR)(\Delta_{\mathbf{R}}\Phi + \Phi\Delta_{\mathbf{R}})]$ . The unpolarized differential cross section is obtained by summing over the different directions of polarization:

$$\frac{d\sigma}{d\Omega}(\mathbf{k} \rightarrow \mathbf{k}') \propto \frac{1}{2} \sum_{\mathbf{g}_{\text{in}}} \sum_{\mathbf{g}_{\text{out}}} |s(\mathbf{g}_{\text{in}}, \mathbf{k} \rightarrow \mathbf{g}_{\text{out}}, \mathbf{k}')|^2. \quad (6)$$

With Eqs. (4)–(6) one obtains the differential cross section of one Rayleigh scatterer in a magneto-optical active matrix for  $k^{-1} \ll R \ll (VB)^{-1}$ :

$$\frac{d\sigma}{d\Omega}(\mathbf{k} \rightarrow \mathbf{k}') \propto U^2 [1 + (\mathbf{k} \cdot \mathbf{k}')^2 + 2(VBR)(\mathbf{k} \cdot \mathbf{k}') \mathbf{k}' \cdot (\mathbf{k} \times \hat{\mathbf{B}})]. \quad (7)$$

Note that the magneto-cross-section depends on  $VBR$ . As  $VBR \gg VB/k$ , this is an *a posteriori* justification of the neglect of the  $VB/k$  term in the potential  $\mathbf{U}$ . The dependence of the magneto-cross-section on the distance  $R$  from the scatterer is somehow surprising. It reflects the fact that the magnetic field acts on the scattered light during all its propagation in the Faraday active medium. As the above considerations are only valid for  $VBR \ll 1$ , this does not

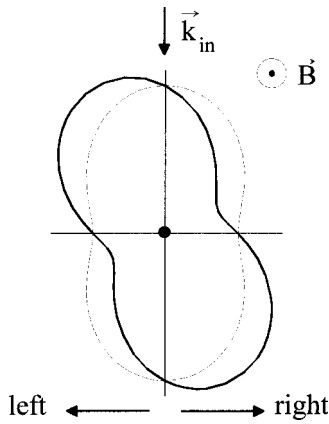


FIG. 7. Polar plot (arb. units) of the differential scattering cross section for one Rayleigh scatterer in the magneto-optical active matrix [cf. Eq. 7]. The wave vector  $\mathbf{k}$  of the incident wave is supposed to be along the vertical axis. The dotted line corresponds to  $B = 0$ . With a magnetic field perpendicular to the plane of the drawing, the cross section gets tilted (solid line) but the integrals over all light scattered to the right and to the left remain equal. So no net magnetotransverse scattering is expected. For better illustration, the parameters were exaggerated:  $VBR = 1$ .

mean that the differential scattering cross section would further increase with the distance. The cross section of Eq. (7) is plotted in Fig. 7. Due to its symmetry, the integrals over the light scattered to the left- and to the right-hand side of the magnetic field are equal. This means that for one single Rayleigh scatterer in a magneto-optical active medium, no net magnetotransverse light flux exists.

However, the situation is different for two Rayleigh scatterers. Let us assume them positioned at  $\mathbf{R}_{1,2} = \pm \mathbf{x}/2$ . The incident wave vector  $\mathbf{k}$  shall be along the interparticle axis and perpendicular to the magnetic field  $\mathbf{B}$ . Because of  $\mathbf{B} \perp \mathbf{k}$ , the incident light wave does not suffer a magneto-phase-shift due to Faraday rotation between the two scatterers. If the mutual separation between the two scatterers well exceeds the wavelength, the two scattering amplitudes simply add coherently. As a consequence, the scattering cross section for the two particles is found to equal the one-particle cross section of Eq. (7) multiplied by an interference factor  $I(\mathbf{k}, \mathbf{k}') = [e^{i(\mathbf{k}-\mathbf{k}') \cdot \mathbf{x}} + e^{-i(\mathbf{k}-\mathbf{k}') \cdot \mathbf{x}}]^2$ . This factor changes the angular profile of the scattering cross section (cf. Fig. 8) and leads to a net magnetotransverse light flux, i.e., to a photonic Hall effect, proportional to  $VBR$ .

This very simple model suggests that the photonic Hall effect for reversed media is due to the influence of the magnetic field on the interference between different light paths. We might assume that in the case of multiple scattering, the  $VBR$  dependence of the photonic Hall effect on  $R$  is trans-

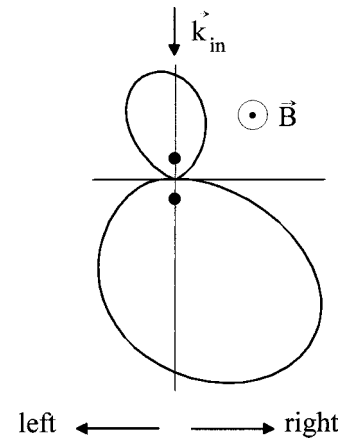


FIG. 8. Polar plot (arb. units) of the differential scattering cross section for two Rayleigh scatterers in distance  $x$  aligned on the vertical axis and in a magneto-optical active surrounding. The wave vector  $\mathbf{k}$  of the incident wave is supposed to be along the vertical axis and a magnetic field is perpendicular to the plane of the drawing. In this case more light is scattered to the right than to the left and a net magnetotransverse scattering is expected. If there were no magnetic field, the cross section would not be tilted and the same amount of light would be scattered to the left and to the right. For better illustration, the parameters were exaggerated:  $VBR = 1$ ;  $kx = 1.2$ .

formed into a  $VB\ell^*$  dependence on the transport mean free path because in multiple scattering  $\ell^*$  is a measure for the distance after which the information about the initial direction of the light has been lost. This is in agreement with our observations.

In conclusion, we have described our observations of the photonic Hall effect in scattering media where the magneto-optical component is the matrix. For these reversed media, our observations exhibit a photonic Hall angle proportional to  $V_m B \ell^*$ . The results of the photonic Hall effect in normal and in reversed media were compared and we have proposed an empirical expression that interpolates the results obtained for the two cases. Finally, we have illustrated the basic physics underlying the reversed photonic Hall effect using a simple analytic model.

## ACKNOWLEDGMENTS

We gratefully acknowledge stimulating discussions with David Lacoste and Peter Wyder. The Grenoble High Magnetic Field Laboratory is a ‘‘laboratoire conventionné aux universités UJF et INP de Grenoble.’’ This research is partially supported by the Groupement de Recherches G 1847 PRIMA of the CNRS in France.

- [1] B.A. van Tiggelen, Phys. Rev. Lett. **75**, 422 (1995).
- [2] B.A. van Tiggelen, R. Maynard, and Th.M. Nieuwenhuizen, Phys. Rev. E **53**, 2881 (1996).
- [3] G.L.J.A. Rikken and B.A. van Tiggelen, Nature (London) **381**, 54 (1996).
- [4] A. Sparenberg, G.L.J.A. Rikken, and B.A. van Tiggelen, Phys.

- Rev. Lett. **79**, 757 (1997).
- [5] N.W. Ashcroft and N.D. Mermin, *Solid State Physics* (Holt, Rinehart and Winston, New York, 1976).
- [6] D. Lacoste and B.A. van Tiggelen, Europhys. Lett. **45**, 721 (1999).
- [7] L.D. Landau, E.M. Lifshitz, and L.P. Pitaevski, *Electrodynam-*

- ics of Continuous Media* (Pergamon, Oxford, 1984).
- [8] G.L.J.A. Rikken, A. Sparenberg, and B.A. van Tiggelen, *Physica B* **246-247**, 188 (1998).
- [9] F. Erbacher, R. Lenke, and G. Maret, *Europhys. Lett.* **21**, 551 (1993).
- [10] R. Lenke, Ph.D. thesis, Université Joseph Fourier, Grenoble, 1994 (unpublished).
- [11] A.S. Martinez and R. Maynard, *Phys. Rev. B* **50**, 3714 (1994).
- [12] H. Senftleben, *Phys. Z.* **XXXI**, 961 (1930); J.M. Beenakker, G. Scoles, H.F.P. Knaap, and R.M. Jonkman, *Phys. Lett.* **2**, 5 (1962); Yu. Kagan and L. Maksimov, *Zh. Éksp. Teor. Fiz.* **41**, 842 (1961) [*Sov. Phys. JETP* **14**, 604 (1962)]; J.P.J. Heemskerk, L.J.F. Hermans, G.F. Bultink, and H.F.P. Knaap, *Physica (Amsterdam)* **57**, 381 (1972).
- [13] R.G. Newton, *Scattering Theory of Waves and Particles* (Springer, New York, 1982).
- [14] D. Lacoste, B.A. van Tiggelen, G.L.J.A. Rikken, and A. Sparenberg, *J. Opt. Soc. Am. A* **15**, 1636 (1998).
- [15] H.C. van de Hulst, *Multiple Light Scattering*, Vol. I & II (Academic, New York, 1980).
- [16] A. Napierala (unpublished).